# Validation of scale-adaptive and elliptic relaxation turbulence models applied to flow around buildings

Christian Heschl [a], Wolfgang Sanz [b], Ines Lindmeier [c], Günter Clauss [d]

[a]*University of Aplied Science,7423 Pinkafeld, AUSTRIA, christian.heschl@fh-burgenland.at*
[b]*Institute for Thermal Turbomachinery and Machine Dynamics, University of Technology 8010 Graz, AUSTRIA, wolfgang.sanz@tugraz.at*
[c]*University of Aplied Science,7423 Pinkafeld, AUSTRIA, christian.heschl@fh-burgenland.at*
[d]*Austrian Wind Power GmbH, 7000 Eisenstadt, AUSTRIA, guenter.clauss@austrianwindpower.com*

ABSTRACT: Computational Fluid Dynamics (CFD) is a commonly accepted tool for studying the wind flow over complex terrain and buildings. But an accurate prediction of the flow field implies a correct reproduction of the turbulent quantities and consequently the right choice of the turbulence model. Due to the highly dissipative behavior of the RANS based turbulence models they are not able to trigger unsteady motion (e.g. flow downstream of buildings) unless the flow instabilities are strong. A more promising assumption is to adjust the turbulence length scale to the local flow inhomogeneities so that the range of the fluctuations resolved is much larger. This approach of a URANS model is denoted Scale-Adaptive Simulation (SAS) and can clearly improve the CFD results for wind flow over complex geometries. Therefore in this work the SST-based Scale-Adaptive Simulation model is investigated by validating it with experimental data from wind tunnel measurements. Beside the SST-SAS model, the standard k-ε and various k-ε-$v^2$-f and k-ω turbulence models are also applied. It shows, that the SST-SAS turbulence model agrees well with the experimental data. But also the k-ε-$v^2$-f turbulence models lead to results of similar quality at lower computational efforts at the same time.

## 1 INTRODUCTION

In the course of the evaluation of wind power resources a detailed prediction of the flow around buildings is necessary. For this Computational Fluid Dynamics (CFD) is often used in the practical design stage. Because of the computational economy the simulations are generally based on the Reynolds-averaged Navier Stokes equations (RANS). Thereby the CFD-user is exposed to the risk of oversimplifying the turbulent processes and consequently he is not able to correctly reproduce the key phenomena encountered in wind and environmental engineering. Especially complex flows such as impingement, bluff body wake and unsteady three dimensional boundary layer separations are affected. The last ones contain geometry induced flow oscillations which can significantly alter the behavior of important parameters such as Reynolds-stresses, turbulent kinetic energy and the dissipation rate (Haase et al., 2009). In principle statistical turbulence models are able to better reproduce such unsteady flows if the turbulence is statistically stationary or if a unique spectral gap which separates the frequency band of the unsteady basic flow from the frequency band of the turbulent fluctuations exists. For the last case unsteady RANS (URANS) models assume that all turbulent fluctuations develop only in the high frequency (low scales) range. Moreover, the unsteady resolved frequency range should lie outside of the modeled turbulence spectrum. In many practical applications both demands are not fulfilled so that an alternative approach to the URANS modeling must be considered.

Because of the deficiencies of the URANS method Spalart et al. (1997) and Strelets (2001) proposed the Detached Eddy Simulation (DES) methodology. DES combines the RANS and Large Eddy Simulation (LES) techniques whereby the turbulent length scale is limited by the grid spacing so that the eddy viscosity is reduced and the three-dimensional turbulent structures in the detached flow region can be directly resolved. The original DES concept was intended for flows with a clear separation of attached and detached flow regions, where the RANS technique would be active in the attached flow region and the LES technique in the detached zone. The use of the LES method leads to high computational costs and to a grid dependency of the results. Motivated by this fact Menter and co-workers (e.g. Menter and Egorov, 2005, 2009) developed a scale-adaptive simulation (SAS) method which uses an additional production term in the ω-equation which considers unsteady effects. For the detecting of the flow unsteadiness the Karman length scale is introduced. The Karman length scale is based on the ratio of the first to the second velocity gradients and is thereby smaller for an unsteady velocity profile than for a steady-state flow (Davidson, 2006). The additional source term contains the ratio between the modeled turbulent length scale and the Karman length scale so that in unsteady flow regions the specific dissipation rate increases and hence the turbulent viscosity decreases. This kind of modification adapts dynamically the standard URANS equations so that more unsteady structures in the flow field can be resolved. Benchmark tests about flow around wall mounted cubes, airfoils, wings, car mirror etc. show that the SAS method can clearly improve the computational results and that this method seems to be a promising alternative to the conventional RANS and URANS approaches (Haase et al., 2009).

To analyze the potential of the SAS model for flow around buildings three different test cases - the flow around a 3D cube, a 3D building array and a 3D hill – were investigated with RANS, URANS and SAS. The used turbulence models depend on the three methods. The RANS models are based on the conventional eddy viscosity concept (EVM) without realizability constraint so that an over production of the turbulent kinetic energy in the stagnation point region arise. Consequently downstream of the obstacles a higher turbulent viscosity can be expected. In contrast to the RANS method all used URANS models include modifications to limit the production of the turbulent kinetic energy in the stagnation point area.

For the RANS and URANS method k-ε and k-ω based turbulence models are used. Past investigations have shown that models which use an elliptic relaxation approach, which accounts for wall blocking effects affecting the Reynolds-stresses, has a very good performance for separated, impinging and bluff body flows (e.g. Lopes da Costa et al., 2007; Sveningsson, 2003; Cokljat et al., 2003; Durbin, 1995a). Therefore k-ε-$v^2$-f based turbulence models are also used for the RANS and URANS calculations. For the SAS investigations only one basis model – the k-ω shear-stress transport model (KW-SST) is used. All simulations were done with the commercial CFD-Code Fluent 12.0.

## 2 DESCRIPTION OF THE APPLIED TURBULENCE MODELS

### 2.1 *Turbulence models for RANS simulation*

The RANS simulations were done with the standard k-ε turbulence model with enhanced wall treatment (SKE) (Fluent, 2009), the k-ω baseline Model (KW-BSL) and the k-ε-$v^2$-f Model (V2F). In contrast to the KW-SST turbulence model the KW-BSL model does not include the adverse pressure gradient correction in the defining equation of the turbulent viscosity. Hence for the KW-BSL model the turbulent viscosity is determined with Eq. (1) and the diffusion coefficient for the transport equation of the turbulent kinetic energy is changed from 1.176 to 2.0 (Menter, 1993).

$$\mu_t = \rho\,\alpha^* \frac{k}{\omega} \tag{1}$$

The V2F Model was implemented in Fluent via user-defined scalar interface (UDS). Because Fluent solves the additional transport equations segregated the code friendly k-ε-$v^2$-f version by Lien and Kalitzin (2001) was used. To avoid singularities in the governing equations at the solid walls the time scale and the length scale is limited by the following equations using Kolmogorov variables:

$$T = \max\left(\frac{k}{\varepsilon}, 6\sqrt{\frac{\nu}{\varepsilon}}\right) \quad L = C_L \max\left(\frac{k^{3/2}}{\varepsilon},\ C_\eta \frac{\nu^{3/4}}{\varepsilon^{1/4}}\right) \tag{2}$$

## 2.2 *URANS based turbulence models*

The URANS simulations are based on the k-ω and k-ε-$v^2$-f Models with realizability constraint to avoid the stagnation point anomaly. For this reason the KW-SST model with the original turbulent viscosity determination (Menter, 1994) was used instead of the KW-BSL model:

$$\mu_t = \frac{\rho\,k}{\omega} \frac{1}{\max\left[\frac{1}{\alpha}, \frac{S\,F_2}{a_1\,\omega}\right]} \tag{3}$$

The k-ε-$v^2$-f Model is extended by the “realizability” constrain proposed by Durbins time scale approach (Durbin, 1995b).

$$T = \min\left[\max\left(\frac{k}{\varepsilon}, 6\sqrt{\frac{\nu}{\varepsilon}}\right), \frac{C_{\lim} k}{\sqrt{6} C_\mu v^2 S}\right] \tag{4}$$

To avoid numerical instabilities the additional limit was only applied in the time scale determination for the turbulent viscosity and the dissipation rate (Sveningsson, 2003). For the model constant $C_{\lim}$ the value $C_{\lim}$=0.6 was assumed. In this paper the k-ε-$v^2$-f Model with the realizability constraint according equation (4) is labeled as V2F-RC.

## 2.3 *SAS based turbulence model*

All SAS simulations were done with the KW-SST based SAS turbulence model included in Fluent 12.0. In this paper the SAS results are denoted as KW-SST-SAS.

# 3 TEST CASES AND RESULTS

To investigate the performance of the RANS, URANS and SAS models the flow over a 3D cube (case A1-4 from the CEDVAL database), a 3D cube array (Brown et al., 2001) and a 3D hill (Ishihara et al., 1999) were chosen due to the abundance of related experimental wind tunnel data. The RANS and URANS calculations reported below were performed with the coupled pressure-based solver and the second order discretization scheme for the convective and unsteady terms. For the SAS calculations the PISO algorithmus was used for the pressure-velocity coupling and the advection was approximated by central-differencing scheme. The near wall grids were arranged so that a $y^+$-value of order 1 of the grid line closest to the wall is achieved. In all simulations the outlet was defined with a pressure, the top side with symmetry and the bottom side with wall boundary condition. For the lateral domain side periodic boundary condition with zero pressure gradients in y-direction were used. To achieve a good convergence behavior the time step size for the URANS simulation was specified at 0.01s and for the SAS model at 0.001s. In both cases the averaging time was about 6 seconds.

## 3.1 *3D Cube*

To ensure a high resolution grid the computational domain consists of 272x143x180 grid cells in the x, y and z direction. The edge length of the cube is H=0.125 m and the computational domain ranges from x/H=-8 upwind and x/H=10 downwind. The height of the domain is limited with z/H=10 and the side boundaries are located at y/H=±5.5H.

The measured velocity distribution at x/H=-8 was used to determine the shear stress velocity ($u_\tau$=0.2916 m/s) and the roughness length ($z_0$=0.000394 m). Based on the logarithmic law the inlet velocity distribution was determined ($u/u_\tau = 1/\kappa \ln (z/z_0)$; Ehrhard, 1999). The turbulent kinetic energy and the dissipation rate were derived from the equilibrium condition between the production and dissipation ($k= u_\tau^2/\mathrm{sqrt}(c_\mu)$ with $c_\mu$=0.09; $\varepsilon= u_\tau^3/ (\kappa\ z)$ and $\omega = u_\tau/ (\kappa\ \mathrm{sqrt}(c_\mu)\ z)$ with $\kappa$=0.4187; Ehrhard, 1999).

Fig. 1 provides a comparison of the predicted and measured x-velocity profiles and the levels of the turbulence kinetic energy downstream of the cube in the y=0 plane. It is surprising that all RANS models (SKE, KW-BSL and V2F) give similar results for both the velocity distribution and the turbulence. The reason for this outcome is the over prediction of the turbulent kinetic energy in the stagnation point as shown in Fig. 2. Consequently the turbulence in the wake is dominated from the stagnation point turbulence transported downstream and suppressing an unsteady solution. On the other hand, if the stagnation point anomaly is corrected as given in Eqs. (3) and (4), no turbulence is generated in the stagnation point region. Thus, less turbulence and thus less numeric dissipation allows the switch into unsteady flow (URANS modeling).

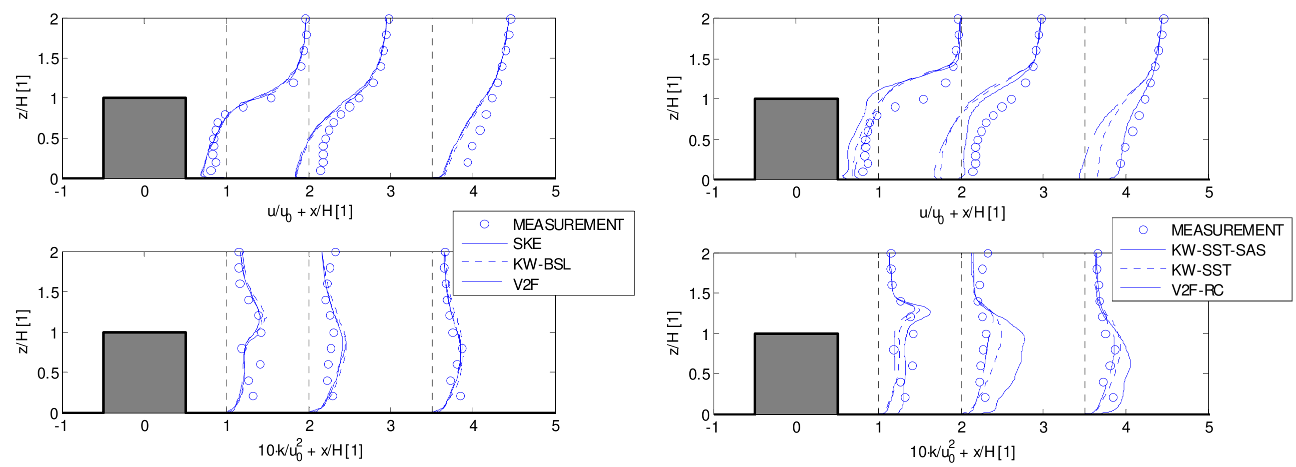


Figure 1. x-velocity and kinetic energy distribution in the y=0 plane downstream of the cube ($u_0$=4.776m/s). Left: investigated RANS models. Right: Investigated URANS and SAS models.

Though the URANS models are able to predict the turbulent kinetic energy distribution more realistic (see Figure 2) the results from the RANS models clearly better agree with the experimental data. It seems that the URANS models are not able to resolve the extent of the unsteady behavior of the basic flow correctly. A reason could be that no spectral gap between the frequency band of the unsteady basic flow and the turbulent fluctuations exists as discussed before.

Immediately downstream of the cube (x/H=1) the RANS models give the best agreement with the experiments, On the other hand, the length of the recirculation zone is clearly overpredicted, because all RANS models underpredict the turbulence kinetic energy (and thus the flow dissipation) in the wake of the obstacle, despite the high turbulence kinetic energy computed in the stagnation point region. So all RANS methods determine the turbulent production in the three dimensional wake insufficiently and overestimate the turbulent dissipation rate.

The additional source term in the KW-SST-SAS model reduces the turbulent viscosity and thus allows larger fluctuations in the wake than the URANS models. Therefore it can capture the flow recovery downstream of the separation zone in good agreement with the experimental data.

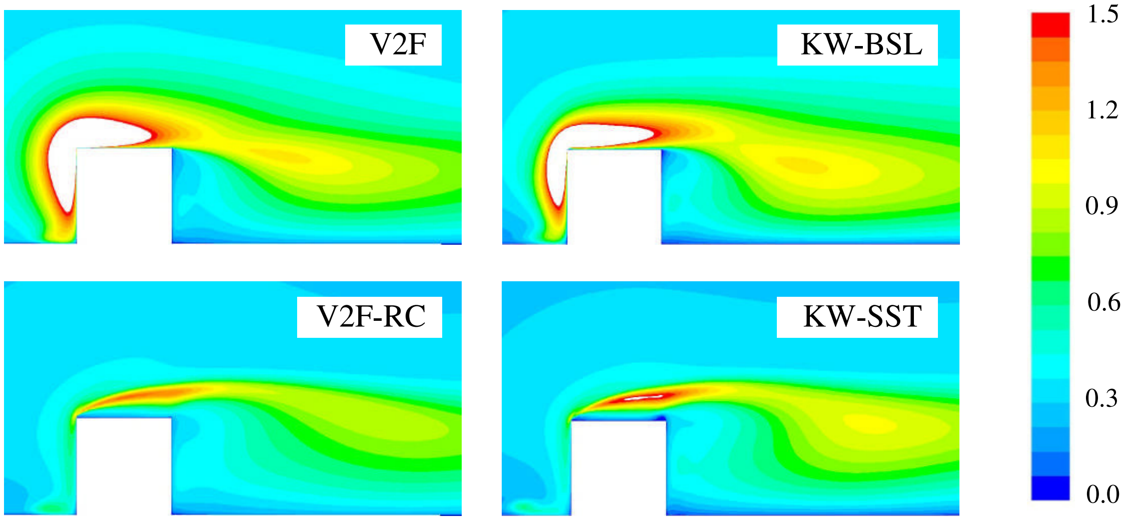


Figure 2. Kinetic energy distribution in the Evaluation plane y=0 (unit of the colorbar [m²/s²]). Top: RANS based models. Bottom: URANS based models.

## 3.2 *3D Array*

A detailed description of the wind tunnel experiments of the flow over a 3D cube array is given by Brown et al. (2001) so that only the important data needed for the computations are presented here. The experiment simulates neutrally stratified atmospheric boundary-layer flow over an array of 3D buildings. The array consists of sharp-edge cubes with a characteristic dimension of H=0.15m. In the experiment 77 cubes were placed in an aligned array consisting of 11 rows of 7 cubes (the arrangement of the cubes is also described in Lien and Yee, 2004). To keep the computational effort low the computational domain was reduced to one row with 7 cubes. The domain spans from x/H=-5 to x/H=23 with the windward face of the first building placed at x/H=0. The height of the domain is z/H=8 and the width y/H=2H. The velocity inlet profile was approximated with the power low $u/u_0=(z/H)^{\alpha}$. According to the experimental data the reference velocity was assumed with $u_0$=3m/s and the exponent with α=0.16. The turbulence parameters for k, ε and ω were derived from the turbulence equilibrium ($k= u_\tau^2/\mathrm{sqrt}(c_\mu)$ with $c_\mu$=0.09; $\varepsilon= u_\tau^3/ (\kappa z)$ and $\omega = u_\tau/ (\kappa\ \mathrm{sqrt}(c_\mu)\ z)$ with κ=0.4187; Ehrhard, 1999). Based on the experiments a friction velocity of $u_\tau$=0.24m/s was used. The number of grid cells was in x-direction 646, in y-direction 82 and in z-direction 98 so that the computational domain consists of about 5 million cells.

Figures 3 to 6 provide a comparison of the predicted velocity profiles in x-direction and the levels of the turbulence kinetic energy. Analogous to the 3D cube all RANS based turbulence models give similar results. In addition both URANS models (KW-SST and V2F-RC) yield similar outcomes to each other. Especially between the first two cubes the RANS models give clearly better results than the URANS and the SAS solution. This corresponds to the observation of the 3D cube case where just behind the trailing edge (x/H=1) URANS and SAS models show also the largest deviations.

However between the cubes 5 and 6 the URANS models agree better with the experimental data. It is assumed that the unsteady behavior of the basic flow there is more distinct from the turbulent fluctuations as between the cubes 1 and 2. The SAS model gives slightly better results than the URANS models there.

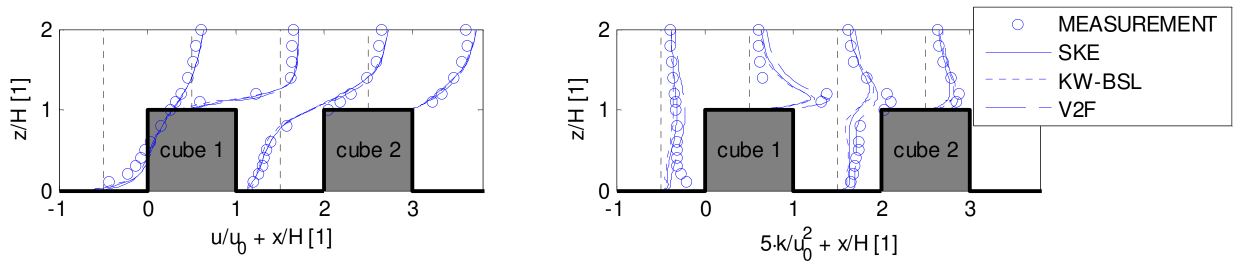


Figure 3. x-velocity and kinetic energy distribution near the cube 1 and 2 (RANS based models).

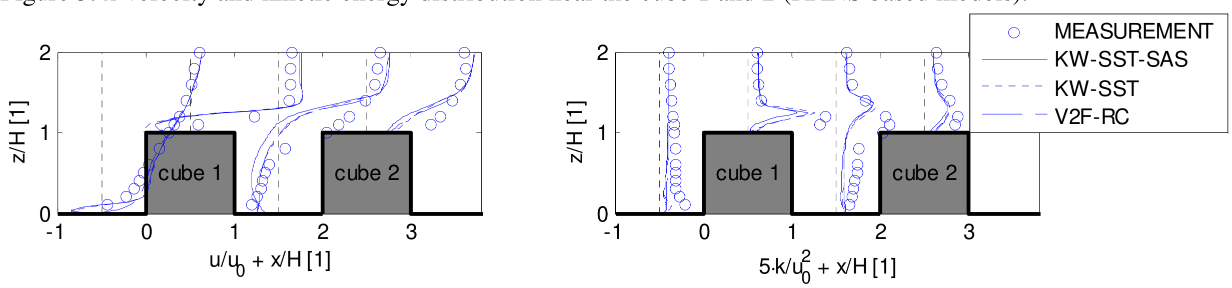


Figure 4. x-velocity and kinetic energy distribution near the cube 1 and 2 (URANS and SAS based models).

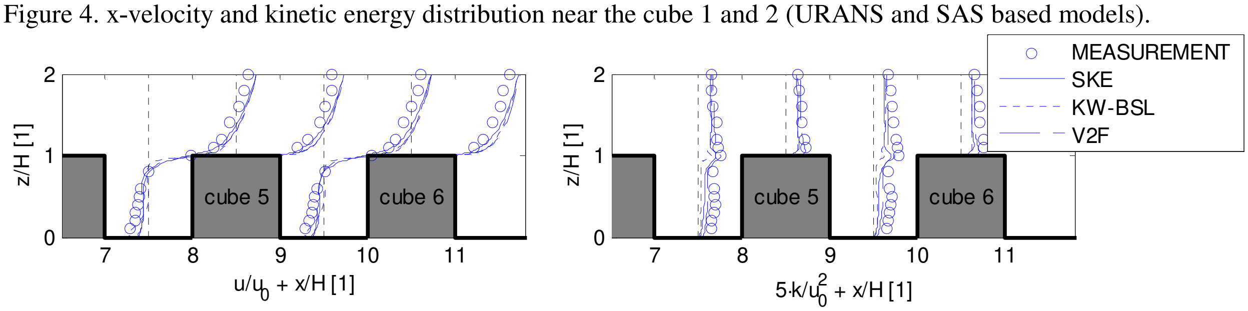


Figure 5. x-velocity and kinetic energy distribution near the cube 5 and 6 (RANS based models).

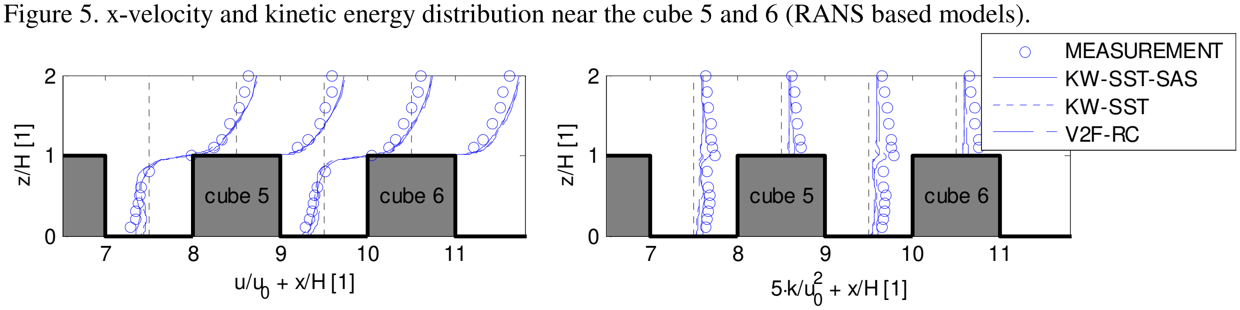


Figure 6. x-velocity and kinetic energy distribution near the cube 5 and 6 (URANS and SAS based models).

### 3.3 *3D Hill*

For the 3D hill test case a mesh with about 2 million cells was used. The origin of the computation domain corresponds to the center of the hill. The inlet was located at x/H=-14 and the outlet at x/H=14. The height of the domain was limited with z/H=12. The periodic planes were defined at y/H=+/-12.5. According to the experimental investigations (Ishihara et al., 1999) the hill height was fixed with H=0.04m and the velocity inlet profile was approximated with the power low $u/u_0=(z/z_0)^\alpha$ ($u_0$=5.5m/s, $z_0$=0.2m and $\alpha$=0.135). The values of the turbulence parameters k, ε and ω were derived from the turbulence equilibrium (equivalent to the 3D cube test case). Based on the experiments a friction velocity of $u_\tau$=0.212m/s was assumed.

The computed results are shown in Figure 7 and 8. In contrast to the other test cases a remarkable difference between the computed results of the different RANS turbulence models can be observed. The results underline the restriction of the SKE model which is not able to reproduce the boundary layer behavior at negative pressure gradients. The comparison between the KW-BSL, the V2F and the URANS as well as the SAS model shows that the RANS based models better agree with the experimental data close to the wall but the transition to the outer flow can be better predicted by the URANS model and the SAS concept. The different distribution of the turbulent kinetic energy and consequently the turbulent viscosity is responsible for the deviations. So the URANS simulations clearly underestimate the turbulent shear stresses near the wall and hence a too large recirculation zone is determined.

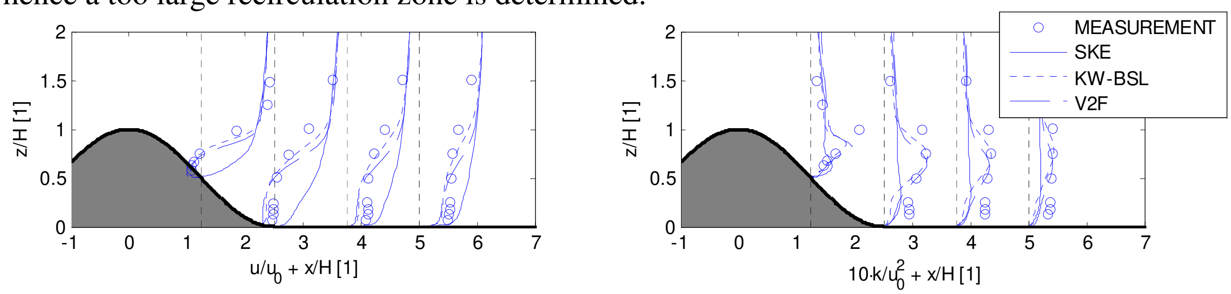


Figure 7. x-velocity and kinetic energy distribution downstream of the hill (RANS based models).

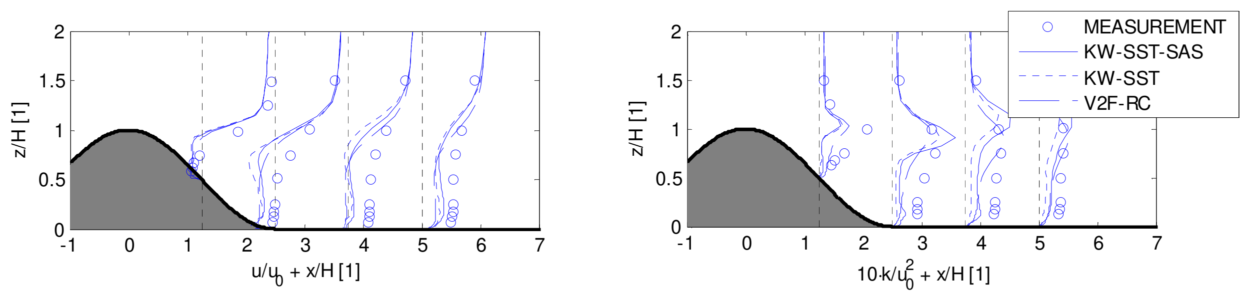


Figure 8. x-velocity and kinetic energy distribution downstream of the hill (URANS and SAS based models).

## 4 CONCLUSIONS

The stagnation point modification for the KW-BSL and the V2F turbulence model was compared with the KW-SST-SAS method. The investigated test cases contained the flow around a three dimensional cube, a cube array and a three dimensional hill. All models without the stagnation point modification produce too much turbulent kinetic energy which is transported downstream and suppressing an unsteady solution. In addition the high turbulence level dominates the turbulent viscosity distribution in the wake so that the used turbulence models (SKE, KW-BSL and V2F) produce similar results. Differences are only observed in the 3D hill test case. In that case the SKE turbulence model fails.

If the stagnation point modification are used the KW-SST and the V2F-RC model switch into unsteady flow (URANS). Compared to the KW-SST-SAS model similar results for the 3D array and the 3D hill are achieved. A significant deviation was only observed in the wake of the 3D cube. In this field the SAS model produces higher velocity fluctuations behind the cube and computes therefore a more realistic recirculation length.

## 5 ACKNOWLEDGEMENTS

The investigations were accomplished by the impulse program "Josef Ressel-Centre" funded by the BMWFJ. Special thanks to Dr. Brown for providing the wind tunnel data.

## 6 REFERENCES

Brown, M., Lawson, R., DeCroix, D., Lee, R., 2001. Comparison of Centerline Velocity Measurements Obtained Around 2D and 3D Arrays in a Wind Tunnel. Report LA-UR-01-4138, Los Alamos National Laboratory, Los Alamos.

CEDVAL http://www.mi.uni-hamburg.de/Data-Sets.432.0.html

Cokljat, D., Kim, S.E., Iaccarino, G., Durbin, P.A., 2003. A comparative assessment of the V2F model for recirculating flows. 41rd AIAA Aerospace Sciences Meeting and Exhibit, Reno, Nevada.

Davidson, L., 2006. Evaluation of the SST-SAS Model: Channel flow, Asymmetric Diffuser and Axi-symmetric Hill. European Conference on Computational Fluid Dynamics, ECCOMAS CFD.

Durbin, P.A., 1995a. Separated flow computations with the $k$-$\varepsilon$-$v^2$ model. AIAA J. 33, 659-664

Durbin, P.A., 1995b. On the $k$-$\varepsilon$ stagnation point anomaly. International Journal of Heat and Fluid Flow, Vol. 17, pp. 89-90.

Ehrhard, J., 1999. Untersuchung linearer und nichtlinearer Wirbelviskositätsmodelle zur Berechnung turbulenter Strömungen um Gebäude, VDI Verlag GmbH, Deutschland.

Fluent, 2009. FLUENT 12.0 User's Guide. Fluent Inc. Centerra Ressource Park, Lebanon.

Haase, W., Braza, M., Revell, A., 2009. DESider – A Euoropean Effort on Hybrid RANS-LES Modelling. Springer, Berlin Heidelberg.

Ishihara, T., Hibi, K., Oikawa, S., 1999. A wind tunnel study of turbulent flow over a three-dimensional steep hill. Journal of Wind Engineering and Industrial Aerodynamics, Vol. 83, 95-107.

Khalighi, B., Zhang, S., Koromilas, C., Balkanyi, S., Bernal, L.P., Iaccarino, G., Moin, P., (2001). Experimental and Computational Study of Unsteady Wake Flow Behind a Bluff Body With a Drag Reduction Device. SAE World Congress, Detroit, MI, USA.

Lien, F., Kalitzin, G., 2001. Computations of transonic flow with the v2f turbulence model. International Journal of Heat and Fluid Flow, Vol. 22, pp. 53-61.

Lien, F., Yee, E., 2004. Numerical modeling of the turbulent flow developing within and over a 3-D building array, Part I: A high-resolution Reynolds-Averaged Navier-Stokes approach. Journal of Boundary-Layer Meteorology 112, 427-466.

Lopes da Costa, J.C., Castro, F.A., Palma, J.M., 2007. Models for Computer Simulation of Wind Flow over Sparsley Forested Regions. Wind Energy, Springer, Berlin Heidelberg.

Menter, F.R., 1993. Zonal Two Equation $k$-$\omega$ Turbulence Models for Aerodynamical Flows. AIAA paper No. 93-2906, 24th Fluid Dynamics Conference, Florida, 1-21.

Menter, F.R., 1994. Two-Equation Eddy-Viscosity Turbulence Models for Engineering Applications. AIAA Journal, Vol. 32, No. 8, pp. 1598 – 1605.

Menter, F.R., Egorov, Y., 2005. A Scale-Adaptive Simulation Model using Two-Equation Models. 43rd AIAA Aerospace Sciences Meeting and Exhibit, Reno, Nevada.

Menter, F.R., Egorov, Y., 2009. Formulation of the Scale-Adaptive Simulation (SAS) Model during the DESIDER Project. In: Haase, W., Braza, M., Revell, A., (eds.). DESider – A Euoropean Effort on Hybrid RANS-LES Modelling. Springer, Berlin Heidelberg.

Spalart, P., Jou, W.-H., Strelets, M., Allmaras, S., 1997. Comments on the feasibility of LES for wings and on the hybrid RANS/LES approach. In: Liu, C., Liu, Z., Sakell, L., (eds.). Advances in DNS/LES, pp. 137-148. Greden Press.

Strelets, M., 2001. Detached Eddy Simulation of massively separated flows. AIAA Paper 2001-879.

Sveningsson, A., 2003. Analysis of the Performance of Different $v^2$-f Turbulence Models in a Stator Vane Passage Flow. PhD thesis, Chalmers University of Technology, Göteborg, Sweden.